AIMS Mathematics, 11(7): 21293–21322.
DOI: 10.3934/math.2026864
Received: 08 April 2026
Revised: 24 June 2026
Accepted: 09 July 2026
Published: 17 July 2026

https://www.aimspress.com/journal/Math

Research article

A model for HPV-related cervical cancer dynamics with saturated terms: an optimal control problem using chemotherapy, immunotherapy, and antibody drugs

Fahad Al Basir[1], **Khalid Aldawsari**[2,*] **and Konstantin B. Blyuss**[3]

[1] Department of Mathematics, Asansol Girls' College, Asansol-4, West Bengal 713304, India

[2] Department of Mathematics, College of Science and Humanities in Al-Kharj, Prince Sattam Bin Abdul Aziz University, Al-Kharj 11942, Saudi Arabia

[3] Department of Mathematics, University of Sussex, Falmer, Brighton BN1 9QH, United Kingdom

* **Correspondence:** Email:k.aldawsari@psau.edu.sa.

Abstract: In this study, we formulate a within-host mathematical model of human papillomavirus (HPV) infection that captures the dynamics of susceptible epithelial cells, infected cells, free virions, cytotoxic T lymphocytes (CTLs), neutralizing antibodies, and cancerous cells. The model incorporates immune mechanisms, including CTL-mediated killing of infected cells and antibody-driven neutralization of virions, as well as therapeutic interventions. Building on this framework, we apply optimal control theory using three treatment strategies: (i) chemotherapy intensity, which enhances infected-cell death and reduces virion production, (ii) CTL stimulation (immunotherapy) intensity, which augments the CTL source term, and (iii) antibody therapy, which strengthens humoral immunity. We first identify the equilibria of the system and test their stability. The disease-free equilibrium is stable when the basic reproduction number is $R_0 < 1$, meaning the infection cannot persist in the population. When $R_0 > 1$, the endemic equilibrium (EE) becomes feasible and is globally asymptotically stable. Finally, the optimal control approach shows that a combined treatment strategy-chemotherapy, immune cell (CTL) boosting, and antibody therapy can significantly minimize viral load and cancer cell growth. This integrated approach demonstrates how traditional chemotherapy and immune-based therapies can complement each other, offering a more effective pathway for managing HPV.

Keywords: within host dynamics; basic reproduction number; sensitivity analysis; optimal control problem; global asymptotic stability; numerical simulations
Mathematics Subject Classification: 91-10, 34D23, 49J15

1. Introduction

Cervical cancer remains one of the leading causes of cancer-related morbidity and mortality among women worldwide, with persistent infection by human papillomavirus (HPV) identified as its primary etiological agent [1]. Despite the availability of prophylactic vaccines and significant advances in therapeutic interventions including surgery, chemotherapy, radiotherapy, immunotherapy, and recombinant gene therapy, the global burden of cervical cancer continues to pose a major public health challenge [2]. The complexity of HPV infection dynamics, coupled with the interplay of host immune responses, necessitates rigorous mathematical modeling to better understand disease progression and to optimize treatment strategies [3].

Chemotherapy remains the cornerstone in the management of advanced cervical cancer [4, 5]. Platinum-based agents, such as cisplatin, have traditionally been the standard, but combination regimens have demonstrated improved outcomes [6]. For instance, topotecan, a semisynthetic derivative of camptothecin, has been found to be effective when combined with cisplatin, resulting in improved overall survival and progression-free survival among patients with recurrent or persistent cervical cancer [7]. Apart from the traditional chemotherapeutic agents, newer approaches include the use of immune checkpoint inhibitors, such as pembrolizumab and nivolumab, and HPV-targeted therapeutic vaccines are under investigation and offer promising avenues of treatment in advanced disease [8]. In concert, these drugs reflect the trend away from conventional cytotoxic agents to targeted and immunological therapies designed to benefit not only survival but also quality of life.

Chemotherapy for cervical cancer often uses platinum-based drugs such as cisplatin or carboplatin. These may be combined with other medicines like paclitaxel, topotecan, or 5-fluorouracil (5-FU) to improve treatment outcomes [9]. In more advanced cases, targeted therapies such as bevacizumab (Avastin) or immunotherapy with pembrolizumab can also be added, often alongside radiation in what is called chemoradiation therapy [10]. Using these treatments in combination helps improve survival rates because they attack the tumor in multiple ways, making the therapy more effective.

Monoclonal antibodies (mAbs) have significantly transformed the treatment of cancers by allowing very targeted approaches that specifically differentiate between malignant and normal cells [11]. mAbs are proteins designed by the laboratory that target antigens found in cancerous cells, hence increasing the immune response, preventing the proliferation of these cells, or releasing toxins that destroy the targeted cancer tissues [12]. Unlike conventional chemotherapeutic agents, which target healthy tissues, mAbs target molecular mechanisms associated with the primary causative agents of cancers, including HER2, CD20, or VEGF, hence increasing their efficiency with little toxicity [13].

Mathematical models have long been employed to study viral infections, providing insights into transmission dynamics, immune system interactions, and therapeutic efficacy [14–16]. However, HPV-specific modeling has largely focused on epidemiological perspectives, with relatively limited attention given to within-host dynamics and the role of immune modulation [3, 17, 18]. In particular, the synergistic effects of cytotoxic T lymphocytes (CTLs) and neutralizing antibodies in controlling HPV infection remain underexplored in formal mathematical frameworks [19].

In this work, we formulate a mathematical model that describes how HPV behaves within the host. The model accounts for several key components: healthy epithelial cells, infected cells, free virus particles, CTLs, antibodies, and cancerous cells. To represent treatment strategies, we introduce three time-dependent control parameters. These correspond to chemotherapy (which increases the

death rate of infected cells and reduces virus production), CTL stimulation through immunotherapy (which boosts CTL generation), and antibody therapy (which enhances antibody production). We analyze the equilibrium states, including both the disease-free and endemic equilibria, and calculate the basic reproduction number of the system. Through numerical simulations, we show how combining chemotherapy, CTL stimulation, and antibody therapy can effectively suppress viral persistence and slow down cancerous cell growth. Finally, this study highlights how integrating immune modulation with direct antiviral effects can provide new insights into optimizing HPV treatment strategies.

2. Model formulation

In this section, we develop a within-host model of HPV infection that captures the dynamics of epithelial cells, free virions, immune responses, and cancerous cells. There are six populations in the model, namely the susceptible epithelial cells $S(t)$, infected epithelial cell $I(t)$, free virions $V(t)$, cancerous cells $C(t)$, CTLs $E(t)$, and antibodies $A(t)$ at any time t.

The model is based on the following assumptions:

(A1) Susceptible epithelial cells $S(t)$ are produced at a constant rate λ and die naturally at rate d_S. They become infected upon contact with free virions at rate β modeled via the saturated term

$$\frac{\beta S V}{1+\sigma V},$$

where σ accounts for saturation effects. Thus, the equation reads as below:

$$\frac{\mathrm{d}S}{\mathrm{d}t} = \lambda - d_S S - \frac{\beta S V}{1+\sigma V}.$$

(A2) Infected epithelial cells $I(t)$ die naturally at rate d_I and are removed through CTL-mediated killing at rate p modeled by the term pEI. Each infected cell produces virions at rate kI with k as the viral replication parameter. Thus, we have

$$\frac{\mathrm{d}I}{\mathrm{d}t} = \frac{\beta S V}{1+\sigma V} - d_I I - pEI.$$

(A3) Free virions $V(t)$ are produced by infected cells at rate k, cleared naturally at rate $d_V V$, and neutralized by antibodies at rate q modeled using the term qAV [20]. Thus, we have

$$\frac{\mathrm{d}V}{\mathrm{d}t} = k\,I - d_V V - qAV.$$

(A4) Cancerous cells $C(t)$ arise from infected cells at rate γ, proliferate at rate ξ, and die at rate d_C with $d_c > \xi$. Thus, the equation for $C(t)$ become

$$\frac{\mathrm{d}C}{\mathrm{d}t} = \gamma\, I + \xi\, C - d_C\, C.$$

(A5) CTLs $E(t)$ enters the system with constant rate s, produced in response to infected cells according to the saturated term

$$\frac{cIE}{h_1+E},$$

and decay naturally at rate d_E [21]. Thus, the dynamics of $E(t)$ is governed by:

$$\frac{\mathrm{d}E}{\mathrm{d}t} = s + \frac{cIE}{h_1 + E} - d_E\, E.$$

(A6) Antibodies $A(t)$ are produced in response to viral load, with antigen-driven stimulation modeled by

$$\frac{\omega VA}{h_2 + A}.$$

They decay at rate $d_A\, A$ and contribute to neutralizing virions and clearing infected cells [22, 23].

From the above assumptions, we finally obtain the following mathematical model:

$$\begin{aligned}
\frac{\mathrm{d}S}{\mathrm{d}t} &= \lambda - d_S S - \frac{\beta S V}{1 + \sigma V},\\
\frac{\mathrm{d}I}{\mathrm{d}t} &= \frac{\beta S V}{1 + \sigma V} - d_I I - pEI,\\
\frac{\mathrm{d}V}{\mathrm{d}t} &= kI - d_V V - qAV,\\
\frac{\mathrm{d}C}{\mathrm{d}t} &= \gamma I + \xi C - d_C C,\\
\frac{\mathrm{d}E}{\mathrm{d}t} &= s + \frac{cIE}{h_1 + E} - d_E E,\\
\frac{\mathrm{d}A}{\mathrm{d}t} &= \frac{\omega VA}{h_2 + A} - d_A A.
\end{aligned} \tag{1}$$

The initial conditions are specified as

$$S(0) > 0, \quad I(0) > 0, \quad V(0) > 0, \quad C(0) > 0, \quad E(0) > 0, \quad A(0) > 0. \tag{2}$$

3. Basic properties of the model

In this section, we establish the nonnegativity and boundedness of solutions to system (1). This ensures the model's biological feasibility. We have also found the system's equilibrium points.

3.1. Nonnegativity and boundedness of solutions

We now establish that the solutions of system (1) subject to the initial conditions (2) remain nonnegative for all $t \geq 0$. The nonnegativity is shown by using the method of contradiction.

Suppose there exists a first time $t_1 > 0$ such that the state variable $S(t)$ becomes negative with other variables being non-negative as per initial conditions, i.e.,

$$I(t) \geq 0, \quad V(t) \geq 0, \quad C(t) \geq 0, \quad E(t) \geq 0, \quad A(t) \geq 0 \quad \text{for } t \in [0, t_1).$$

Then at t_s, that variable must satisfy

$$S(t_1) = 0.$$

Thus from the equation of S, we have

$$\frac{\mathrm{d}S}{\mathrm{d}t} = \lambda \geq 0.$$

Hence, $S(t)$ cannot cross into negative values, which contradicts our assumption.

Again, assume that $t_2 > 0$ is the first time $I(t)$ becomes negative with other nonnegative variables. Thus, at $t = t_2$, we have

$$\frac{\mathrm{d}I}{\mathrm{d}t} = \frac{\beta S(t_2)V(t_2)}{1 + \sigma V(t_2)} \geq 0.$$

This shows that $I(t)$ cannot cross the negative axis. This is again a contradiction. Thus, $I(t)$ is nonnegative for all $t > 0$.

Similarly, we can show the nonnegativity for remaining model variables.

Therefore, the system (1) with initial conditions (2) is biologically wellposed, and all state variables remain nonnegative throughout the evolution of the model.

Boundedness: From the first equation of the model (1), we have

$$\frac{\mathrm{d}S}{\mathrm{d}t} = \lambda - d_S S - \frac{\beta S V}{1 + \sigma V} \leq \lambda - d_S S.$$

Solving this, we can write

$$0 \leq S(t) \leq \max\left\{S(0), \frac{\lambda}{d_S}\right\}. \tag{3}$$

From the second equation of (1) and using

$$\frac{V}{1 + \sigma V} \leq \frac{1}{\sigma},$$

and $S(t) \leq \bar{S}$, we get

$$\frac{\mathrm{d}I}{\mathrm{d}t} = \frac{\beta S V}{1 + \sigma V} - d_I I - pEI \leq \frac{\beta \bar{S}}{\sigma} - d_I I.$$

This gives the following inequality:

$$0 \leq I(t) \leq \max\left\{I(0), \frac{\beta \bar{S}}{\sigma d_I}\right\}. \tag{4}$$

From the third equation, we can write

$$\frac{\mathrm{d}V}{\mathrm{d}t} = kI - d_V V - qAV \leq kI - d_V V \leq k\bar{I} - d_V V.$$

This gives

$$0 \leq V(t) \leq \max\left\{V(0), \frac{k\bar{I}}{d_V}\right\}. \tag{5}$$

Considering the fourth equation of (1) and using

$$\frac{E}{h_1 + E} \leq 1,$$

we have

$$\frac{\mathrm{d}E}{\mathrm{d}t} = s + \frac{cIE}{h_1 + E} - d_E E \leq s + cI - d_E E \leq s + c\bar{I} - d_E E,$$

hence,

$$0 \leq E(t) \leq \max\left\{E(0), \frac{s + c\bar{I}}{d_E}\right\}. \tag{6}$$

Using

$$\frac{A}{h_2 + A} \leq 1,$$

from fifth equation, we have

$$\frac{\mathrm{d}A}{\mathrm{d}t} = \frac{\omega VA}{h_2 + A} - d_A A \leq \omega\, V - d_A A \leq \omega\, \bar{V} - d_A A.$$

Therefore,

$$0 \leq A(t) \leq \max\left\{A(0), \frac{\omega\bar{V}}{d_A}\right\}. \tag{7}$$

Using the last equation of system (1), we obtain

$$\frac{\mathrm{d}C}{\mathrm{d}t} = \gamma I + \xi C - d_C C = \gamma I - (d_C - \xi)C.$$

Now,

$$\frac{\mathrm{d}C}{\mathrm{d}t} \leq \gamma\bar{I} - (d_C - \xi)\, C,$$

and hence

$$0 \leq C(t) \leq \max\left\{C(0), \frac{\gamma\bar{I}}{d_C - \xi}\right\}, \tag{8}$$

since $d_C > \xi$ (according to the assumption (A4)).

From the above discussion, we have the following theorem.

Theorem 1. *The compact set*

$$\mathcal{B} := \left\{(S, I, V, C, E, A) \in \mathbb{R}^6_{\geq 0} :\ 0 \leq S \leq \tilde{S},\ 0 \leq I \leq \tilde{I},\ 0 \leq V \leq \tilde{V},\ 0 \leq C \leq \tilde{C},\ 0 \leq E \leq \tilde{E},\ 0 \leq A \leq \tilde{A}\right\}, \tag{9}$$

where $d_C > \xi$ and

$$\tilde{S} = \max\left\{S(0), \frac{\lambda}{d_S}\right\}, \quad \tilde{I} = \max\left\{I(0), \frac{\beta\tilde{S}}{\sigma d_I}\right\}, \quad \tilde{V} = \max\left\{V(0), \frac{k\tilde{I}}{d_V}\right\},$$

$$\tilde{E} = \max\left\{E(0), \frac{s + c\tilde{I}}{d_E}\right\}, \quad \tilde{A} = \max\left\{A(0), \frac{\omega\tilde{V}}{d_A}\right\}, \quad \tilde{C} = \max\left\{C(0), \frac{\gamma\tilde{I}}{d_C - \xi}\right\},$$

is positively invariant, and all trajectories with initial data (2) *remain in $\mathcal{B}$ for all $t \geq 0$.*

Remark 1. *The bound on C naturally requires $d_C > \xi$. This is a biologically reasonable assumption (cytokine clearance dominates net production feedback). Without it, C may exhibit unbounded growth driven by positive linear feedback, even if the other compartments are bounded.*

3.2. Equilibrium points

The model (1) has two equilibria, namely:

(i) The disease-free equilibrium (DFE), $U_0\left(\frac{\lambda}{d_S}, 0, 0, 0, \frac{s}{d_E}, 0\right)$,

(ii) The endemic equilibrium (EE) given by $U^*(S^*, I^*, V^*, C^*, U^*, A^*)$, where

$$
\begin{aligned}
S^* &= \frac{\lambda\omega}{d_S\omega + (\sigma d_S + \beta)d_A(A^* + h_2)},\\
I^* &= \frac{d_V + qA^*}{k\sigma}\left(\frac{\beta\lambda k}{(d_V + qA^*)(d_I + pE^*)M} - 1\right),\\
V^* &= \frac{kI^*}{d_V + qA^*},\\
C^* &= \frac{\gamma I^*}{d_C - \xi},\\
E^* &= \frac{d_I}{p}\left(\frac{\beta\lambda k}{d_I(d_V + qA^*)M} - 1\right),
\end{aligned}
$$

with

$$
M = \left(d_S + \frac{(\sigma d_S + \beta)d_A(A^* + h_2)}{\omega}\right),
$$

and A^* is the positive root of the quartic polynomial in A^*:

$$
a_4(A^*)^4 + a_3(A^*)^3 + a_2(A^*)^2 + a_1A^* + a_0 = 0, \tag{10}
$$

with coefficients:

$$
\begin{aligned}
a_4 &= d_I^2\, d_E\, q^2\, \frac{(\sigma d_S + \beta)\, d_A}{\omega},\\
a_3 &= -2\, d_I^2\, d_E\, q\, d_V\, \frac{(\sigma d_S + \beta)\, d_A}{\omega} - c\, \frac{d_A}{\omega}\, q^2\, d_I,\\
a_2 &= d_I^2\, d_E(d_V^2 + \frac{2qd_Vh_2d_A}{\omega}) - \frac{cd_Aqd_Vd_I}{\omega} - spq\, \frac{(\sigma d_S + \beta)\, d_A}{\omega},\\
a_1 &= -2\, d_Id_Ed_Vh_1p - \frac{cd_Ad_V^2d_I}{\omega} - spd_V\, \frac{(\sigma d_S + \beta)d_A}{\omega},\\
a_0 &= (\beta\lambda\, k - d_Id_Vd_S)\left(d_E(h_1p + \beta\,\lambda\, k - d_Id_Vd_S) - \frac{cd_Ah_2d_V}{\omega}\right) - sp(h_1\, p + \beta\lambda k - d_Id_Vd_S).
\end{aligned}
$$

We note that $a_4 > 0, a_3 < 0$, and $a_1 < 0$. Thus, we have the following results.

Proposition 1. *Consider the quartic polynomial* (10) *with coefficients a_4, a_3, a_2, a_1, a_0 defined as above.*
(i) The polynomial admits at least one positive real root if $a_0 < 0$,
(ii) If both $a_2 < 0$ and $a_0 < 0$, then there exists a unique positive root of (10).

3.3. The basic reproduction number

The basic reproduction number R_0 is a threshold parameter that determines whether the infection can invade and persist in the host. To compute R_0, we employ the next generation matrix (NGM) method [24] focusing on the infection subsystem involving infected epithelial cells $I(t)$ and free virions $V(t)$.

Other compartments such as $S(t)$, $C(t)$, $E(t)$, and $A(t)$ do not directly generate new infections and are therefore excluded from the NGM construction.

We now separate the dynamics of $I(t)$ and $V(t)$ into two components: (i) the new infection terms, denoted by $\mathcal{F}$, which represent the appearance of new infections, (ii) the transition terms, denoted by $\mathcal{V}$, which represent all other changes (natural death, clearance, immune removal). Thus, we can write

$$\mathcal{F} = \begin{bmatrix} \dfrac{\beta S V}{1+\sigma V} \\ kI \end{bmatrix}, \qquad \mathcal{V} = \begin{bmatrix} d_I I + pEI \\ d_V V + qAV \end{bmatrix}.$$

At the DFE, there are no infected cells or virions:

$$I = 0, \quad V = 0, \quad C = 0.$$

The susceptible cell population is given by

$$\bar{S} = \frac{\lambda}{d_S},$$

while the CTL population settles at its baseline value

$$\bar{E}* = \frac{s}{d_E}, \quad A^* = 0.$$

We compute the Jacobians of $\mathcal{F}$ and $\mathcal{V}$ with respect to the infected compartments (I, V) at the DFE. For $\mathcal{F}$, we have

$$F = \begin{bmatrix} 0 & \dfrac{\beta S^*}{1+\sigma\cdot 0} \\ k & 0 \end{bmatrix} = \begin{bmatrix} 0 & \dfrac{\beta\lambda}{d_S} \\ k & 0 \end{bmatrix}.$$

For $\mathcal{V}$, we get

$$V = \begin{bmatrix} d_I + pE^* & 0 \\ 0 & d_V + qA^* \end{bmatrix} = \begin{bmatrix} d_I + \dfrac{ps}{d_E} & 0 \\ 0 & d_V \end{bmatrix}.$$

The next generation matrix is defined as

$$K = FV^{-1}.$$

Substituting the matrices, we obtain the next generation matrix as

$$K = \begin{bmatrix} 0 & \dfrac{\beta\lambda}{d_S d_V} \\ \dfrac{k}{d_I + \dfrac{ps}{d_E}} & 0 \end{bmatrix}.$$

The eigenvalues ρ of K satisfy

$$\rho^2 = \frac{\beta\lambda}{d_S d_V} \cdot \frac{k}{d_I + \frac{ps}{d_E}}.$$

Hence, the basic reproduction number is given by the spectral radius of K:

$$R_0 = \sqrt{\frac{\beta k \lambda}{d_S d_V \left(d_I + \frac{ps}{d_E}\right)}}. \tag{11}$$

Remark 2. *The expression for R_0 highlights the balance between viral replication and immune clearance. The numerator involves the infection rate β, viral production rate k, and the supply of susceptible cells λ, all of which promote infection. The denominator involves the death rate of susceptible cells d_S, the clearance rate of virions d_V, and the combined removal of infected cells through natural death and CTL-mediated killing*

$$\left(d_I + \frac{ps}{d_E}\right),$$

all of which suppress infection. This helps in proposing control interventions.

Remark 3. *We obtained*

$$R_0 = \sqrt{\frac{\beta k \lambda}{d_S d_V \left(d_I + \frac{ps}{d_E}\right)}}$$

as the basic reproduction number of system (1)*. Now, if $R_0 > 1$, then the EE exists and satisfies*

$$I^* = \frac{(d_V + qA^*)}{k\sigma}\left(\frac{\beta\lambda k}{(d_V + qA^*)(d_I + pE^*)\left(d_S + \frac{(\sigma d_S + \beta)d_A(A^* + h_2)}{\omega}\right)} - 1\right) > 0.$$

Hence, the infected cell population is strictly positive whenever $R_0 > 1$. Similarly, E^* is also positive when $R_0 > 1$. Thus, if $R_0 < 1$, the infection cannot establish and will eventually die out, whereas if $R_0 > 1$, the infection persists within the host.

4. Stability of equilibria

We analyze the stability of equilibria in the following subsections.

4.1. Stability of DFE

The DFE is $U_0(\frac{\lambda}{d_S}, 0, 0, 0, \frac{s}{d_E}, 0)$. The Jacobian matrix at U_0 is determined as:

$$J_{U_0} = \begin{bmatrix} -d_S & 0 & -\frac{\beta\lambda}{d_S} & 0 & 0 & 0 \\ 0 & -d_I - \frac{ps}{d_E} & \frac{\beta\lambda}{d_S} & 0 & 0 & 0 \\ 0 & k & -d_V & 0 & 0 & 0 \\ 0 & \gamma & 0 & -(d_C - \xi) & 0 & 0 \\ 0 & 0 & 0 & 0 & -d_E & 0 \\ 0 & 0 & 0 & 0 & 0 & -d_A \end{bmatrix}.$$

The eigenvalues are

$$\mu_1 = -d_S, \quad \mu_2 = -d_E, \quad \mu_3 = -d_A, \quad \mu_4 = -(d_C - \xi),$$

and the remaining satisfy the following equation:

$$H(\mu) = \mu^2 + \mu\left(d_I + \frac{ps}{d_E} + d_V\right) + d_V\left(d_I + \frac{ps}{d_E}\right) - \frac{\beta\lambda k}{d_S} = 0.$$

By the Routh-Hurwitz criterion, both roots of $H(\mu)$ have negative real parts if

$$d_V(d_I + \frac{ps}{d_E}) - \frac{\beta\lambda k}{d_S} > 0,$$

i.e., if $R_0 < 1$.

Also, using (9), we have $\mu_4 < 0$. Therefore, the DFE is locally asymptotically stable if $R_0 < 1$. Thus we have the following theorem.

Theorem 2. *The DFE is locally asymptotically stable if $\mathcal{R}_0 < 1$ and unstable if $\mathcal{R}_0 > 1$. Consequently, forward bifurcation occurs at $R_0 = 1$.*

Proof of the first part of the theorem is directly followed by the above discussion. For the proof of the last part, one can see [25].

Remark 4. *Biologically, $\mathcal{R}_0 < 1$ implies that each infected cell produces fewer than one secondary infection on average, leading to eventual eradication of the virus. Conversely, $\mathcal{R}_0 > 1$ indicates sustained viral replication and potential epidemic outbreaks. Thus, interventions that reduce transmission (β), enhance clearance (d_V), or increase immune removal (θ_I) are critical for controlling infection.*

4.2. Local stability of EE

The Jacobian matrix of the system at the EE, $U^*(S^*, I^*, V^*, C^*, E^*, A^*)$ is

$$J = [J_{ij}] = \begin{bmatrix} -d_S - \frac{\beta V^*}{1+\sigma V^*} & 0 & -\frac{\beta S^*}{(1+\sigma V^*)^2} & 0 & 0 & 0 \\ \frac{\beta V^*}{1+\sigma V^*} & -d_I - pE^* & \frac{\beta S^*}{(1+\sigma V^*)^2} & 0 & -pI^* & 0 \\ 0 & k & -d_V - qA^* & 0 & 0 & -qV^* \\ 0 & \gamma & 0 & \xi - d_C & 0 & 0 \\ 0 & \frac{cE^*}{h_1+E^*} & 0 & 0 & \frac{cI^*h_1}{(h_1+E^*)^2} - d_E & 0 \\ 0 & 0 & \frac{\omega A^*}{h_2+A^*} & 0 & 0 & \frac{\omega V^* h_2}{(h_2+A^*)^2} - d_A \end{bmatrix}.$$

The characteristic equation is

$$P(\mu) = (\mu + \xi - d_C) \cdot (\mu^5 + a_1\mu^4 + a_2\mu^3 + a_3\mu^2 + a_4\mu + a_5) = 0, \tag{12}$$

where the coefficients are given below:

$$\begin{aligned}
a_1 &= -(J_{11} + J_{22} + J_{33} + J_{55} + J_{65}),\\
a_2 &= J_{11}(J_{22} + J_{33} + J_{55} + J_{65}) + J_{22}(J_{33} + J_{55} + J_{65}) + J_{33}(J_{55} + J_{65})\\
&\quad + J_{55}(J_{65} - J_{63}) - J_{23}J_{32} - J_{24}J_{52} - J_{35}J_{63},\\
a_3 &= -\Big[J_{11}\Big(J_{22}J_{33}J_{55} - J_{22}J_{35}J_{63} - J_{23}J_{32}J_{55} + J_{23}J_{35}J_{63} - J_{24}J_{52}J_{33}\\
&\quad + J_{22}J_{33}J_{65} - J_{23}J_{32}J_{65} + J_{22}J_{55}J_{65} - J_{24}J_{52}J_{65} + J_{33}J_{55}J_{65} - J_{35}J_{63}J_{55}\Big)\\
&\quad - J_{11}J_{13}J_{21}J_{32} + J_{22}\Big(J_{33}J_{55}J_{65} - J_{35}J_{63}J_{55}\Big)\\
&\quad - J_{23}J_{32}J_{55}J_{65} + J_{23}J_{35}J_{52}J_{65} - J_{24}J_{52}J_{33}J_{65} + J_{24}J_{52}J_{35}J_{63}\Big],\\
a_4 &= J_{11}\Big(J_{22}J_{33}(J_{55} + J_{65}) - J_{22}J_{35}J_{63} - J_{23}J_{32}(J_{55} + J_{65}) + J_{23}J_{35}J_{63}\\
&\quad + J_{24}J_{32}J_{55} + J_{24}J_{52}(J_{35} - J_{33} - J_{65})\Big) + J_{13}\Big(J_{21}J_{32}(J_{55} + J_{65}) - J_{21}J_{35}J_{63} - J_{22}J_{35}J_{52}\Big)\\
&\quad + J_{55}\Big(J_{22}J_{33}J_{65} - J_{22}J_{35}J_{63} - J_{23}J_{32}J_{65} + J_{23}J_{35}J_{63}\Big)\\
&\quad + J_{65}\Big(J_{22}J_{33}J_{55} - J_{23}J_{32}J_{55} - J_{24}J_{52}J_{33}\Big) + J_{55}J_{65}(J_{22} + J_{33}),\\
a_5 &= -\Big[J_{11}\Big(J_{22}J_{33}J_{55}(J_{65} - J_{63}) - J_{22}J_{35}J_{55}J_{63} - J_{23}J_{32}J_{55}(J_{65} - J_{63}) + J_{23}J_{35}J_{52}J_{65}\\
&\quad - J_{24}J_{32}J_{55}J_{65} + J_{24}J_{52}(J_{33}J_{65} - J_{35}J_{65} + J_{35}J_{63})\Big)\\
&\quad - J_{13}\Big(J_{21}J_{32}J_{55}(J_{65} - J_{63}) - J_{21}J_{35}J_{52}(J_{65} - J_{63}) + J_{22}J_{35}J_{52}(J_{65} - J_{63})\Big)\Big].
\end{aligned}$$

Applying Routh-Hurwitz criteria on

$$\mu^5 + a_1\mu^4 + a_2\mu^3 + a_3\mu^2 + a_4\mu + a_5 = 0,$$

we get the stability conditions as:

$$\begin{aligned} &\text{i.} \quad a_1 > 0,\ a_5 > 0,\ a_1a_2 - a_3 > 0, \\ &\text{ii.} \quad a_3(a_1a_2 - a_3) - a_1(a_1a_4 - a_5) > 0, \\ &\text{iii.} \quad a_4[a_3(a_1a_2 - a_3) - a_1(a_1a_4 - a_5)] - a_5[a_2(a_1a_2 - a_3) - (a_1a_4 - a_5)] > 0. \end{aligned} \tag{13}$$

Equation (12) has a negative root $-(d_C - \xi)$, and the rest of the roots have negative real parts if Eq (13) is satisfied. Thus, the EE E^* is stable if the above conditions given in Eq (13) are satisfied.

5. Global stability of the EE

We construct the following Volterra-type Lyapunov function:

$$\begin{aligned} L = {} & \alpha_S\left(S - S^* - S^*\ln\frac{S}{S^*}\right) + \alpha_I\left(I - I^* - I^*\ln\frac{I}{I^*}\right) \\ & + \alpha_V\left(V - V^* - V^*\ln\frac{V}{V^*}\right) + \alpha_C\left(C - C^* - C^*\ln\frac{C}{C^*}\right) \\ & + \alpha_E\left(E - E^* - E^*\ln\frac{E}{E^*}\right) + \alpha_A\left(A - A^* - A^*\ln\frac{A}{A^*}\right), \end{aligned} \tag{14}$$

where $\alpha_i > 0$, $i = S, I, V, C, E, A$.

Clearly,

$$L \geq 0,$$

and

$$L = 0 \quad \Longleftrightarrow \quad (S, I, V, C, E, A) = (S^*, I^*, V^*, C^*, E^*, A^*).$$

Differentiating L along the trajectories of system (1), we obtain

$$\begin{aligned} \dot{L} = {} & \alpha_S\left(1 - \frac{S^*}{S}\right)\left(\lambda - d_S S - \frac{\beta S V}{1 + \sigma V}\right) \\ & + \alpha_I\left(1 - \frac{I^*}{I}\right)\left(\frac{\beta S V}{1 + \sigma V} - d_I I - pEI\right) \\ & + \alpha_V\left(1 - \frac{V^*}{V}\right)(kI - d_V V - qAV) \\ & + \alpha_C\left(1 - \frac{C^*}{C}\right)(\gamma I + \xi C - d_C C) \\ & + \alpha_E\left(1 - \frac{E^*}{E}\right)\left(s + \frac{cIE}{h_1 + E} - d_E E\right) \\ & + \alpha_A\left(1 - \frac{A^*}{A}\right)\left(\frac{\omega V A}{h_2 + A} - d_A A\right). \end{aligned} \tag{15}$$

At the EE $U^* = (S^*, I^*, V^*, C^*, E^*, A^*)$, the following relations hold:

$$\begin{aligned} \lambda &= d_S S^* + \frac{\beta S^* V^*}{1+\sigma V^*}, \\ \frac{\beta S^* V^*}{1+\sigma V^*} &= (d_I + pE^*) I^*, \\ kI^* &= (d_V + qA^*) V^*, \\ \gamma I^* + \xi C^* &= d_C C^*, \\ s + \frac{cI^* E^*}{h_1 + E^*} &= d_E E^*, \\ \frac{\omega V^* A^*}{h_2 + A^*} &= d_A A^*. \end{aligned} \tag{16}$$

Using (16), we derive

$$T_1 = \left(1 - \frac{S^*}{S}\right)\left(\lambda - d_S S - \frac{\beta S V}{1+\sigma V}\right) = -d_S \frac{(S-S^*)^2}{S} + \left(1 - \frac{S^*}{S}\right)\left(\frac{\beta S^* V^*}{1+\sigma V^*} - \frac{\beta S V}{1+\sigma V}\right), \tag{17}$$

$$T_2 = \left(1 - \frac{I^*}{I}\right)\left(\frac{\beta S V}{1+\sigma V} - (d_I + pE)I\right) = \left(1 - \frac{I^*}{I}\right)\left(\frac{\beta S V}{1+\sigma V} - \frac{\beta S^* V^*}{1+\sigma V^*}\right) - (d_I + pE)\frac{(I-I^*)^2}{I}, \tag{18}$$

$$\left(1 - \frac{V^*}{V}\right)(kI - (d_V + qA)V) = kI\left(1 - \frac{V^*}{V}\right) - (d_V + qA)\frac{(V-V^*)^2}{V}, \tag{19}$$

$$T_3 = \left(1 - \frac{C^*}{C}\right)(\gamma I + \xi C - d_C C) = \gamma\left(1 - \frac{C^*}{C}\right)(I - I^*) - d_C \frac{(C-C^*)^2}{C}, \tag{20}$$

$$T_4 = \left(1 - \frac{E^*}{E}\right)\left(s + \frac{cIE}{h_1 + E} - d_E E\right) = \left(1 - \frac{E^*}{E}\right)\left[\frac{cIE}{h_1 + E} - \frac{cI^* E^*}{h_1 + E^*}\right] - d_E \frac{(E-E^*)^2}{E}, \tag{21}$$

and

$$T_5 = \left(1 - \frac{A^*}{A}\right)\left(\frac{\omega V A}{h_2 + A} - d_A A\right) = \left(1 - \frac{A^*}{A}\right)\left[\frac{\omega V A}{h_2 + A} - \frac{\omega V^* A^*}{h_2 + A^*}\right] - d_A \frac{(A-A^*)^2}{A}. \tag{22}$$

We choose $\alpha_S = \alpha_I = \alpha_C = \alpha_E = \alpha_A = 1$, and

$$\alpha_V = \frac{\beta S^* V^*}{kI^*(1+\sigma V^*)}.$$

Substituting $T_i,\ i = 1, 2, 3, 4, 5$ into (15), we obtain

$$\begin{aligned} \dot{L} = &-d_S \frac{(S-S^*)^2}{S} - (d_I + pE)\frac{(I-I^*)^2}{I} \\ &- \alpha_V (d_V + qA)\frac{(V-V^*)^2}{V} - d_C \frac{(C-C^*)^2}{C} \\ &- d_E \frac{(E-E^*)^2}{E} - d_A \frac{(A-A^*)^2}{A} + \Phi, \end{aligned} \tag{23}$$

where

$$\begin{aligned}\Phi = &\left(1-\frac{S^*}{S}\right)\left(\frac{\beta S^* V^*}{1+\sigma V^*}-\frac{\beta S V}{1+\sigma V}\right)+\left(1-\frac{I^*}{I}\right)\left(\frac{\beta S V}{1+\sigma V}-\frac{\beta S^* V^*}{1+\sigma V^*}\right)\\ &+\alpha_V k I\left(1-\frac{V^*}{V}\right)+\left(1-\frac{E^*}{E}\right)\left[\frac{cIE}{h_1+E}-\frac{cI^*E^*}{h_1+E^*}\right]\\ &+\left(1-\frac{A^*}{A}\right)\left[\frac{\omega VA}{h_2+A}-\frac{\omega V^*A^*}{h_2+A^*}\right]+\gamma\left(1-\frac{C^*}{C}\right)(I-I^*).\end{aligned} \tag{24}$$

Using the choice of α_V, the infection terms cancel exactly:

$$\left(1-\frac{S^*}{S}\right)\left(\frac{\beta S^* V^*}{1+\sigma V^*}-\frac{\beta S V}{1+\sigma V}\right)+\alpha_V\, k\, I\left(1-\frac{V^*}{V}\right)=0.$$

Next, we estimate the nonlinear immune-response terms. Since

$$f(E)=\frac{E}{h_1+E}$$

is increasing for $E>0$, by the mean value theorem,

$$(\frac{IE}{h_1+E}-\frac{I^*E^*}{h_1+E^*})(I-I^*)\geq 0.$$

Hence,

$$\left(1-\frac{E^*}{E}\right)\left[\frac{cIE}{h_1+E}-\frac{cI^*E^*}{h_1+E^*}\right]\leq\frac{c}{h_1}\,|I-I^*|\,|E-E^*|. \tag{25}$$

Similarly,

$$g(A)=\frac{A}{h_2+A}$$

is increasing for $A>0$, and thus

$$\left(1-\frac{A^*}{A}\right)\left[\frac{\omega VA}{h_2+A}-\frac{\omega V^*A^*}{h_2+A^*}\right]\leq\frac{\omega}{h_2}\,|V-V^*|\,|A-A^*|. \tag{26}$$

Also,

$$\gamma\left(1-\frac{C^*}{C}\right)(I-I^*)\leq\gamma\,|I-I^*|\,|C-C^*|. \tag{27}$$

Applying Young's inequality,

$$ab\leq\frac{\varepsilon a^2}{2}+\frac{b^2}{2\varepsilon},$$

to the inequalities (25)–(27), we can write from (24)

$$\begin{aligned}\Phi\leq&\frac{c}{2h_1}\left[\varepsilon_1(I-I^*)^2+\frac{1}{\varepsilon_1}(E-E^*)^2\right]\\ &+\frac{\omega}{2h_2}\left[\varepsilon_2(V-V^*)^2+\frac{1}{\varepsilon_2}(A-A^*)^2\right]\\ &+\frac{\gamma}{2}\left[\varepsilon_3(I-I^*)^2+\frac{1}{\varepsilon_3}(C-C^*)^2\right].\end{aligned} \tag{28}$$

Therefore,

$$\dot{L} \leq 0,$$

provided that the parameters satisfy

$$\begin{aligned} d_I + pE &> \frac{c\varepsilon_1}{2h_1} + \frac{\gamma\varepsilon_3}{2}, \\ d_E &> \frac{c}{2h_1\varepsilon_1}, \\ \alpha_V(d_V + qA) &> \frac{\omega\varepsilon_2}{2h_2}, \\ d_A &> \frac{\omega}{2h_2\varepsilon_2}, \\ d_C &> \frac{\gamma}{2\varepsilon_3} \end{aligned} \tag{29}$$

for some positive constants $\varepsilon_1, \varepsilon_2, \varepsilon_3 > 0$.

Hence, $\dot{L} \leq 0$ in $\mathcal{B}$. Moreover, $\dot{L} = 0$ if and only if

$$S = S^*,\ I = I^*,\ V = V^*,\ C = C^*,\ E = E^*,\ A = A^*.$$

Therefore, the largest invariant subset of $\left\{\dot{L} = 0\right\}$ is the singleton $\{U^*\}$.

By LaSalle's invariance principle, every solution trajectory in $\mathcal{B}$ approaches the endemic equilibrium U^* as $t \to \infty$. Thus,

$$(S(t),\ I(t),\ V(t),\ C(t),\ E(t),\ A(t)) \to (S^*,\ I^*,\ V^*,\ C^*,\ E^*,\ A^*) \tag{30}$$

as $t \to \infty$.

Hence, the EE U^* is globally asymptotically stable in $\mathcal{B}$. Thus, we have the following theorem.

Theorem 3. *For initial conditions in $\mathcal{B}$, as long as parameters satisfy conditions (29), the endemic steady state U^* is globally asymptotically stable in $\mathcal{B}$, with all solutions satisfying*

$$(S(t),\ I(t),\ V(t),\ C(t),\ E(t),\ A(t)) \to U^* \quad \text{as } t \to \infty,$$

for any

$$(S(0),\ I(0),\ V(0),\ C(0),\ E(0),\ A(0)) \in \mathcal{B}.$$

6. Optimal control problem

To investigate treatment strategies for HPV infection, we introduce three time-dependent control variables. The first control, denoted by $u_1(t)$, represents chemotherapy intensity, which acts by increasing the death rate of infected cells and reducing virion production. The second control, $u_2(t)$, corresponds to CTL stimulation (immunotherapy) intensity, which augments the source term of CTLs and thereby strengthens the cellular immune response. The third control, $u_3(t)$, models antibody therapy intensity, which enhances antibody production and contributes to virion neutralization. Each control function $u_i(t)$, for $i = 1, 2, 3$, is bounded between 0 and 1, ensuring that the treatment levels remain within biologically feasible limits [26].

The controlled system is then described by the following nonlinear differential equations:

$$\begin{aligned}
\frac{dS}{dt} &= \lambda - d_S S - \frac{\beta S V}{1+\sigma V},\\
\frac{dI}{dt} &= \frac{\beta S V}{1+\sigma V} - d_I I - pEI,\\
\frac{dV}{dt} &= kI - d_V V - qAV - \theta_V\, u_1(t)\, V,\\
\frac{dC}{dt} &= \gamma I + \xi C - d_C C - \theta_C\, u_2(t)\, C,\\
\frac{dE}{dt} &= s + \frac{cIE}{h_1+E} - d_E E,\\
\frac{dA}{dt} &= \mu u_3(t) + \frac{\omega V A}{h_2+A} - d_A A,
\end{aligned} \tag{31}$$

with initial conditions (2).

The objective is to minimize both infection burden and viral load while penalizing excessive treatment effort. We define the cost functional:

$$J(u_1,u_2,u_3) = \int_0^{t_f} \left(w_1 I(t) + w_2 V(t) + \frac{1}{2}B_1 u_1^2(t) + \frac{1}{2}B_2 u_2^2(t) + \frac{1}{2}B_3 u_3^2(t)\right) \mathrm{d}t, \tag{32}$$

where w_1 and w_2 are positive weights reflecting the importance of reducing infected cells and viral load, while B_1, B_2, B_3 are penalty constants associated with the intensity of chemotherapy, CTL stimulation, and antibody therapy, respectively.

We define the admissible control set as

$$\mathcal{U} = \{(u_1(t),u_2(t),u_3(t)) : 0 \le u_i(t) \le 1, \text{ are measurable}, i = 1,2,3\}. \tag{33}$$

The optimal control problem is therefore to determine measurable functions $u_1^*(t)$, $u_2^*(t)$, $u_3^*(t)$ satisfying $0 \le u_i(t) \le 1$, $i = 1,2,3$ that minimize the cost functional (32) subject to the state system (31). Mathematically, the problem is to find $(u_1^*, u_2^*, u_3^*) \in \mathcal{U}$ such that

$$J(u_1^*,u_2^*,u_3^*) = \inf_{(u_1,u_2,u_3)\in\mathcal{U}} J(u_1,u_2,u_3), \tag{34}$$

subject to the state system (31).

6.1. Characterization of the optimal control

The Hamiltonian for the minimization problem is assumed as

$$\begin{aligned}
H = {} & w_1 I + w_2 V + w_3 C + \frac{1}{2}B_1 u_1^2 + \frac{1}{2}B_2 u_2^2 + \frac{1}{2}B_3 u_3^2\\
& + \lambda_1\left(\lambda - d_S S - \frac{\beta S V}{1+\sigma V}\right)\\
& + \lambda_2\left(\frac{\beta S V}{1+\sigma V} - d_I I - pEI\right)\\
& + \lambda_3\left(kI - d_V V - qAV - \theta_V\, u_1\, V\right)
\end{aligned} \tag{35}$$

$$
\begin{aligned}
&+ \lambda_4 (\gamma I + \xi C - d_C C - \theta_C u_2 C) \\
&+ \lambda_5 \left(s + \frac{cIE}{h_1 + E} - d_E E \right) \\
&+ \lambda_6 \left(\mu u_3 + \frac{\omega V A}{h_2 + A} - d_A A \right),
\end{aligned}
$$

where $\lambda_1(t), \lambda_2(t), \lambda_3(t), \lambda_4(t), \lambda_5(t)$, and $\lambda_6(t)$ are introduced as adjoint variables. According to Pontryagin's maximum principle [27], the adjoint equations are given by

$$
\dot{\lambda}_j = -\frac{\partial H}{\partial x}, \quad x \in \{S,\ I,\ V,\ C,\ E,\ A\},\ \text{i=1,2,...,6.} \tag{36}
$$

Using (36), we derive the adjoint system as

$$
\begin{cases}
\dot{\lambda}_1 &= -(-d_S \lambda_1 - \dfrac{\beta V}{1+\sigma V}\lambda_1 + \dfrac{\beta V}{1+\sigma V}\lambda_2), \\
\dot{\lambda}_2 &= -(w_1 + k\lambda_3 + \gamma\lambda_4 + \dfrac{cE}{h_1+E}\lambda_5 - d_I\lambda_2 - pE\lambda_2), \\
\dot{\lambda}_3 &= -(w_2 - \dfrac{\beta S}{(1+\sigma V)^2}\lambda_1 + \dfrac{\beta S}{(1+\sigma V)^2}\lambda_2 - d_V\lambda_3 - qA\lambda_3 + \dfrac{\omega A}{h_2+A}\lambda_6 - \theta_V u_1\,\lambda_3), \\
\dot{\lambda}_4 &= -(w_3 + (\xi - d_c - \theta_C u_2)\lambda_4), \\
\dot{\lambda}_5 &= -(-pI\lambda_2 + \dfrac{cIh_1}{(h_1+E)^2}\lambda_5 - d_E\lambda_5), \\
\dot{\lambda}_6 &= -(-qV\lambda_3 + \dfrac{\omega V h_2}{(h_2+A)^2}\lambda_6 - d_A\lambda_6),
\end{cases} \tag{37}
$$

with boundary condition $\lambda_i(t_f) = 0$.

Now, we determine the control parameters. By Pontryagin's maximum principle [27], the optimal controls are characterized by the minimization of the Hamiltonian with respect to each control variable. This yields the condition

$$
\frac{\partial H}{\partial u_i} = 0, \quad i = 1,\ 2,\ 3 \tag{38}
$$

together with the admissible bounds $0 \le u_i(t) \le 1$. Projecting onto the admissible control set, the optimal controls are therefore given by

$$
\begin{cases}
u_1^*(t) = \min\{1,\ \max\{0,\ \dfrac{\theta_V\, V(t)\, \lambda_3(t)}{B_1}\}\}, \\
u_2^*(t) = \min\{1,\ \max\{0,\ \dfrac{\theta_C\, C(t)\, \lambda_4(t)}{B_2}\}\}, \\
u_3^*(t) = \min\{1,\ \max\{0,\ -\dfrac{\mu\, \lambda_6(t)}{B_3}\}\}.
\end{cases} \tag{39}
$$

Thus, the optimal control problem contains the state system (31), adjoint system (37), and optimal control triplet (39). Hence, it is a two-point boundary value problem.

For the numerical simulations, the optimality system was solved using the forward–backward sweep method implemented in MATLAB. The state equations were solved forward in time using a fourth-order Runge-Kutta scheme, while the adjoint equations were solved backward in time using the same discretization method. The controls were initially guessed as constant functions satisfying

$$u_1^{(0)}(t) = u_2^{(0)}(t) = u_3^{(0)}(t) = 0$$

for all $t \in [0, t_f]$. At each iteration, the controls were updated using the characterization Eq (39). The iterative process was terminated when the maximum absolute difference between successive control iterates satisfied

$$\max_{i=1,2,3} \|u_i^{(k+1)} - u_i^{(k)}\|_\infty < 10^{-6}.$$

The time interval $[0, t_f]$ was discretized using a uniform step size $\Delta t = 0.01$.

7. Sensitivity analysis

To investigate the impact of model parameters on the basic reproduction number (R_0), we compute the forward sensitivity index ($\Upsilon_\theta^{R_0}$) using R_0 with respect to the generic parameter θ as follows:

$$\Upsilon_\theta^{R_0} = \frac{\partial R_0}{\partial \theta} \cdot \frac{\theta}{R_0}. \tag{40}$$

In this study, we derive R_0 as

$$R_0 = \sqrt{\frac{\beta\lambda k}{d_S(d_V + q\omega)\left(d_I + \dfrac{ps}{d_E}\right)}}. \tag{41}$$

The sensitivity indices are obtained using (40) as follows:

$$\Upsilon_\beta^{R_0} = \Upsilon_\lambda^{R_0} = \Upsilon_k^{R_0} = +\frac{1}{2}, \quad \Upsilon_{d_S}^{R_0} = -\frac{1}{2}, \quad \Upsilon_{d_E}^{R_0} = +\frac{1}{2} \cdot \frac{ps/d_E}{d_I + ps/d_E},$$

$$\Upsilon_{d_V}^{R_0} = -\frac{1}{2} \cdot \frac{d_V}{d_V + q\omega}, \quad \Upsilon_q^{R_0} = -\frac{1}{2} \cdot \frac{q\omega}{d_V + q\omega}, \quad \Upsilon_\omega^{R_0} = -\frac{1}{2} \cdot \frac{q\omega}{d_V + q\omega},$$

$$\Upsilon_{d_I}^{R_0} = -\frac{1}{2} \cdot \frac{d_I}{d_I + \dfrac{ps}{d_E}}, \quad \Upsilon_p^{R_0} = -\frac{1}{2} \cdot \frac{ps/d_E}{d_I + ps/d_E}, \quad \Upsilon_s^{R_0} = -\frac{1}{2} \cdot \frac{ps/d_E}{d_I + ps/d_E}.$$

The measure is defined by the percentage change of R_0 with a percentage change of parameter x. This index allows one to assess the impact of sensitivity among the different parameters in a normalized manner. A 10% increase in β leads to a 5% increase in R_0, due to the square root property. An increase of 10% in d_V causes a decrease in R_0 of 5%. An increase in d_E has a significant effect on R_0, indicating that the model is sensitive to immune clearance. One can conclude that R_0 is sensitive to changes in β, k, and λ, and also the immune clearance rate.

8. Numerical simulations

In this section, we present the numerical simulations using the values of parameters as in Table 1. We vary important parameters to observe their impact on the system. Finally, we plot the solutions of the optimal system.

Table 1. Model parameters, values, and references for HPV infection dynamics with chemotherapy and CTL activator drugs.

Short description	Symbol	Baseline value	Reference
Susceptible cell recruitment rate	λ	5×10^6	[28]
Susceptible cell death rate	d_S	0.1	[29]
Infection rate per virion	β	5×10^{-7}	[1,28]
Infected cell death rate	d_I	2.0	[2]
CTL killing rate of infected cells	p	0.01	[30]
Virion production rate per infected cell	k	50	[3]
Virion clearance rate	d_V	0.5	[30]
Basal CTL source rate	s	0.5	[30]
CTL proliferation rate	c	10^{-2}	[18]
CTL decay rate	d_E	0.12	[18]
Maximal antibody production rate	ω	0.3	[19]
Half-saturation constant	h_1	100	[19]
Antibody decay rate	d_A	0.1	[19]
Virion neutralization rate by antibodies	q	1×10^{-3}	[19]
Antibody-mediated clearance of infected cells	α	5×10^{-4}	[19]

In Figure 1, sensitivity indices are plotted. From this figure, we observe that the parameters β, λ, and k have equal positive sensitivity 0.5, whereas removal processes (d_S, d_V, q, ω, d_I, p, s) have negative sensitivity. Interestingly, the CTL decay rate (d_E) exhibits a positive sensitivity, highlighting its role in weakening immune control when increased. This figure emphasizes the most influential parameters of the system. The biological and therapeutic factors in HPV infection dynamics are identified. Positive values indicate that an increase in the parameter leads to an increase in R_0, while negative values indicate a reduction in R_0. To obtain a disease-free system, we need $R_0 < 1$. Thus, the parameters that reduce R_0 should be increased to manage the disease or vice versa.

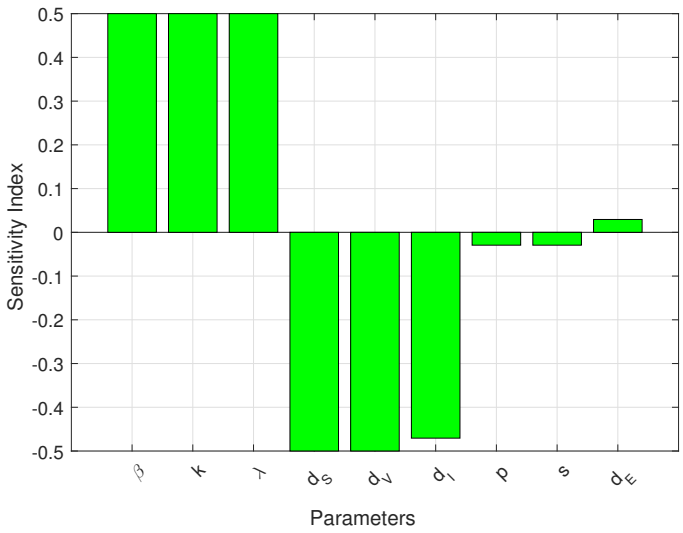

Figure 1. Sensitivity indices of model parameters are plotted using the values as in Table 1.

Figure 2 contains the region of stability of the DFE. For lower values of the infection rate β and viral replication rate k, the DFE is stable as the basic reproduction number R_0 is below unity. Also, as the infected cell killing rate p increases, the region of stability increases. This shows p has a stabilizing role in the system.

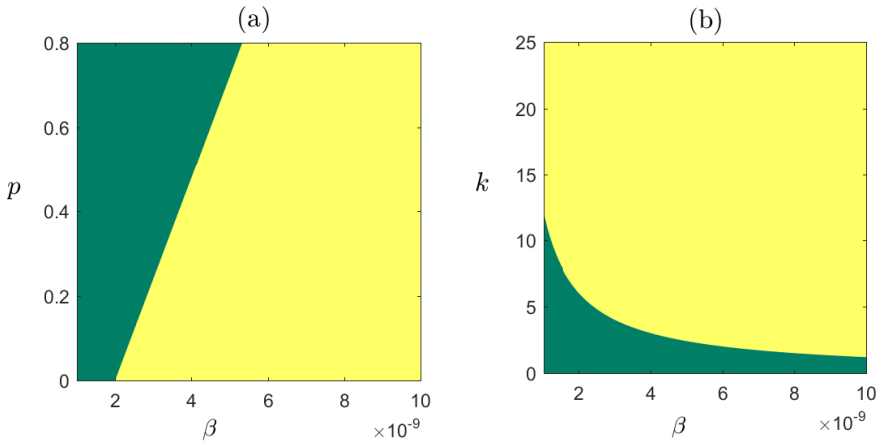

Figure 2. Region of stability of the DFE U_0 in (a) $\beta - p$ and (b) $\beta - k$ planes. Other parameter values are taken from Table 1. In the yellow region, U_0 is unstable and stable in green regions.

In Figure 3, we show the solutions when the basic reproduction is less than unity and when the basic reproduction number is greater than unity. When infection rate is lower ($\beta = 0.2 \times 10^{-9}$), the infected cells and virus population become zero as $R_0 < 1$. When the rate is comparatively higher ($\beta = 5 \times 10^{-8}$), $R_0 = 1.625 > 1$, and the system becomes endemic. The EE is asymptotically stable in this parametric situation.

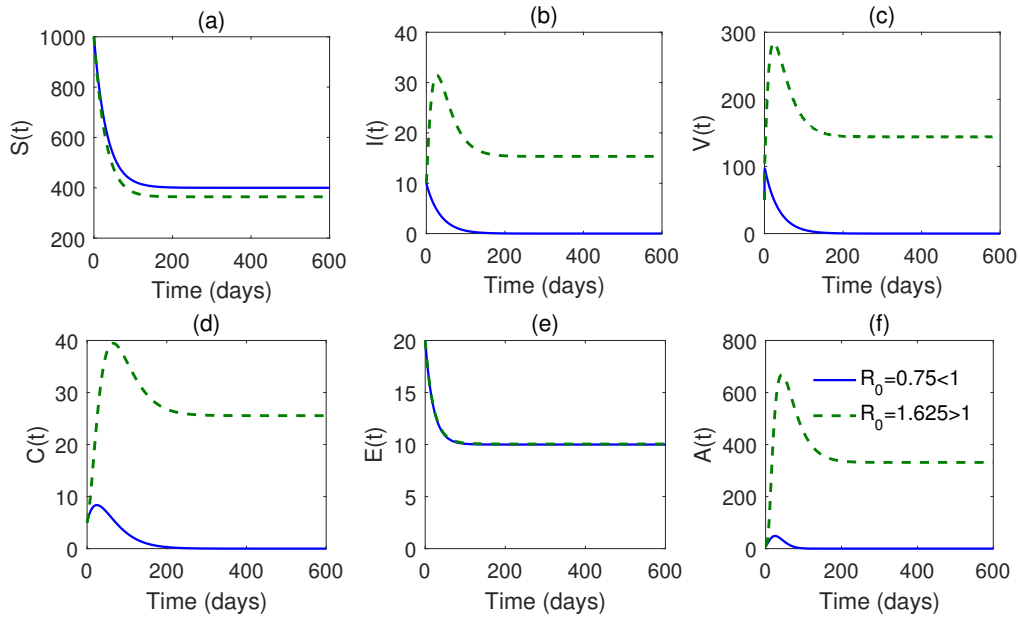

Figure 3. Time series solution of the system for $R_0 < 1$ (blue lines) and $R_0 > 1$ (green dashed lines). Parameter values are taken from Table 1, except $\beta = 0.0001$ (blue lines) and $\beta = 0.0005$ (green lines).

In Figure 4, we explore how changes in the infection rate affect the steady-state levels of infected cells and viral population, plotted against the basic reproduction number. The DFE is stable when $R_0 < 1$, but it loses stability once $R_0 > 1$. At the critical threshold $R_0 = 1$, the system undergoes a forward transcritical bifurcation. Beyond this point, with $R_0 > 1$, the system settles into an endemic state. Put simply, the infection rate must exceed a certain threshold for the system to sustain endemicity.

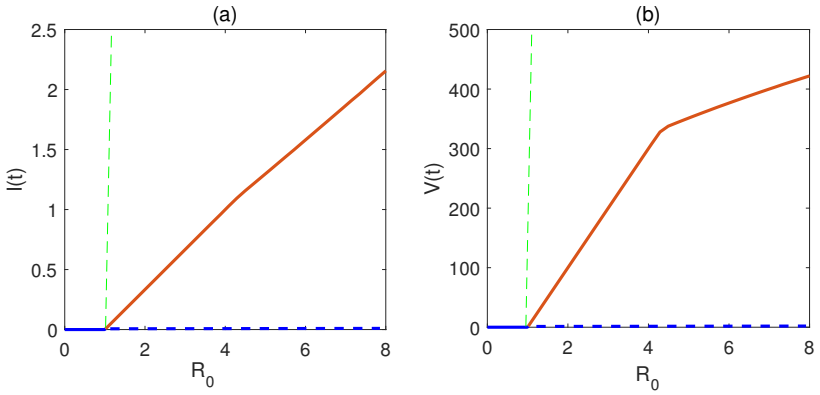

Figure 4. Forward bifurcation: Steady state values of the infected cell and virus population are plotted vs R_0. Here, β is varied, and other parameter values are taken from Table 1. Solid blue lines represent stable DFE, and blue dashed lines indicate unstable DFE. Red lines represent stable EE.

Phase portraits are plotted for three different initial conditions in Figure 5. Each trajectory converges to the same steady point, the EE. This shows the nonlinear stability of the EE. Biologically, this indicate

that the infection will persist but settle into a steady state.

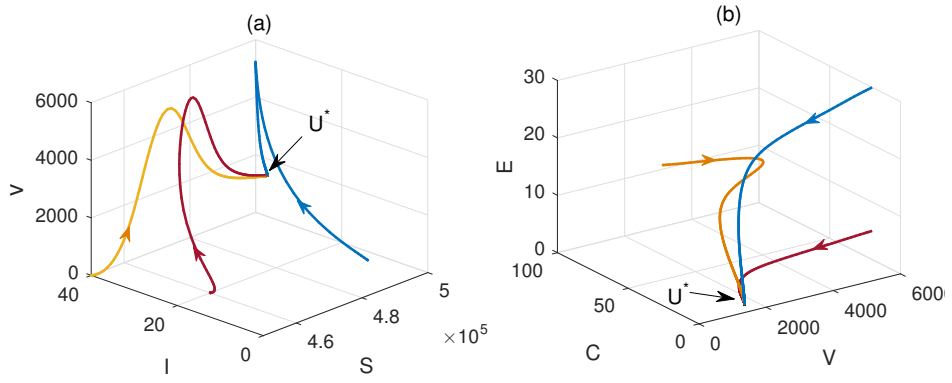

Figure 5. Phase trajectories plotted for different initial values in (a) $S-I-V$, and (b) $V-C-E$ phase spaces. Parameter values are kept the same as in Table 1.

The effects of varying parameters ω, p, and q are illustrated in Figures 6–9, respectively. Increasing the values of these parameters leads to a reduction in infection, as evidenced by the decreasing levels of infected cells, viral load, and cancerous cells. Based on these findings, we subsequently implement the optimal treatment strategy.

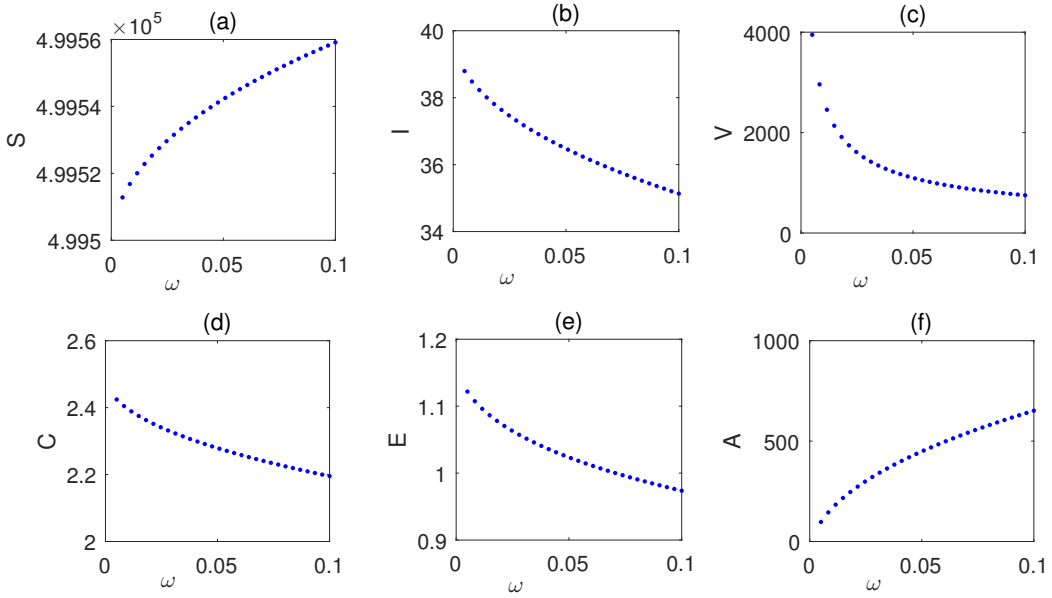

Figure 6. Effect of ω on the steady state values of model populations. Other parameter values are the same as in Table 1.

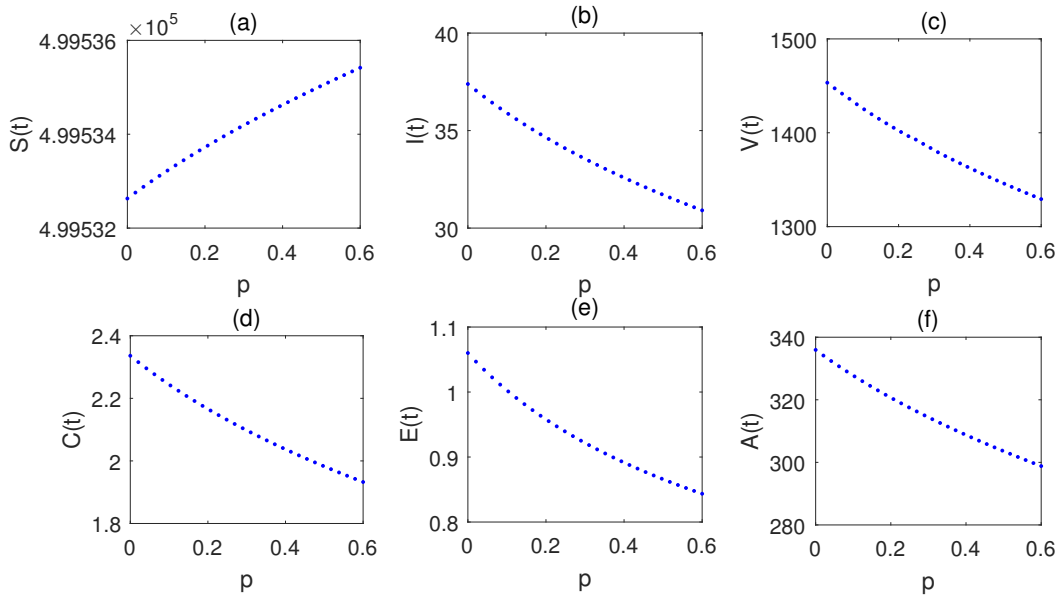

Figure 7. Effect of p on the steady state values of model populations. Parameter values are kept the same as in Table 1.

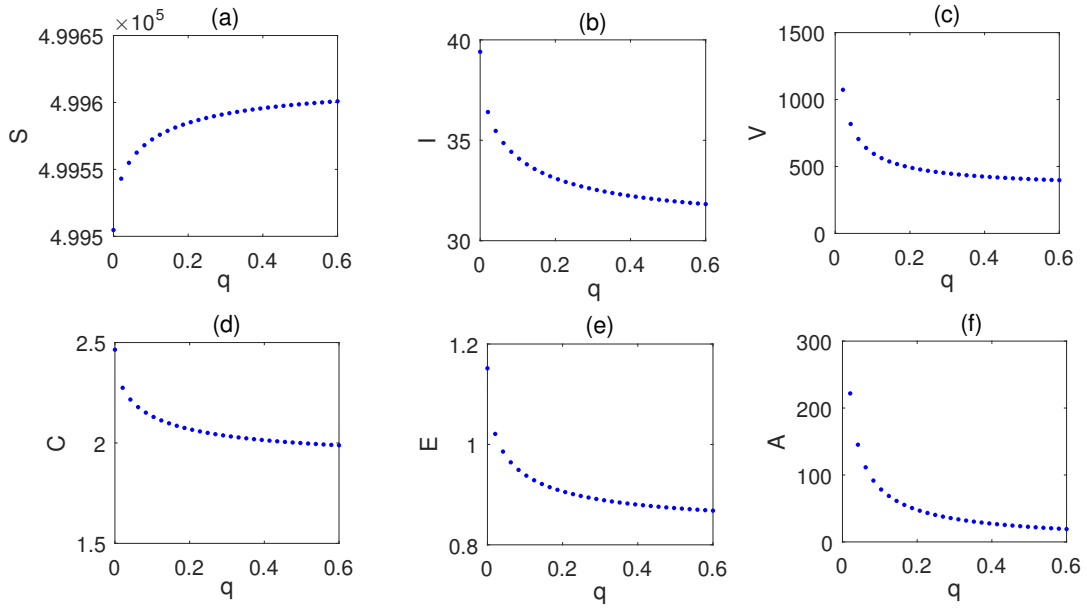

Figure 8. Effect of q on the steady state values of model populations. Parameter values are kept same as in Table 1.

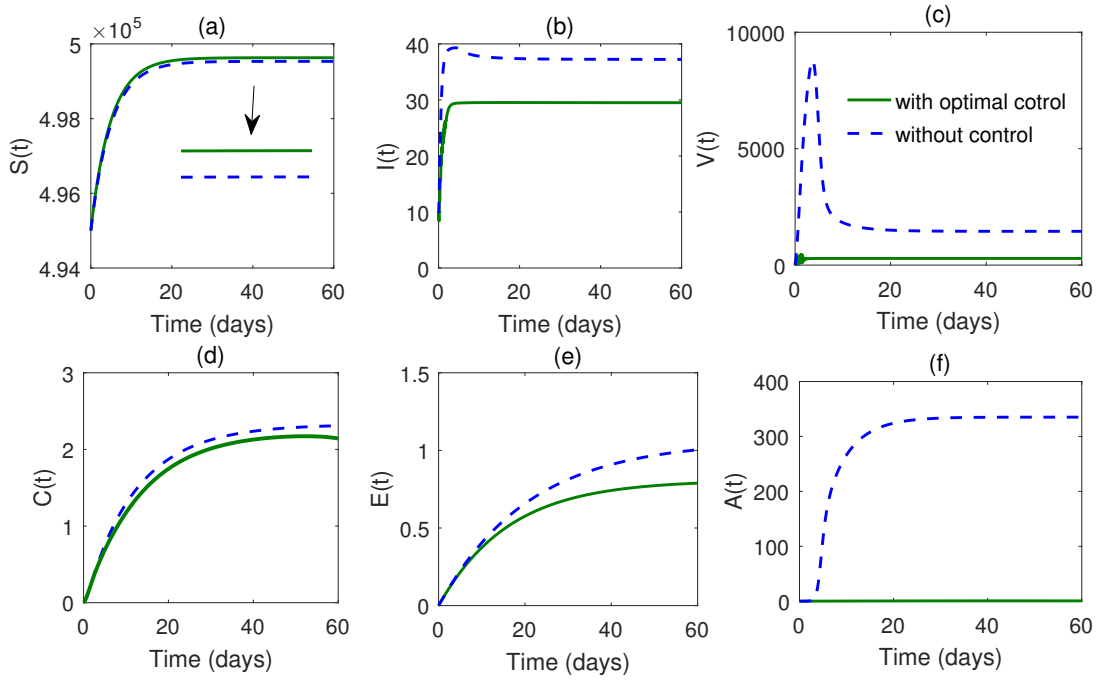

Figure 9. The systems with control and without control are compared. Parameter values are taken from Table 1.

The optimality system is solved numerically using a Matlab forward–backward sweep method, which provides an efficient iterative scheme for optimal control problems. In this approach, the state system (31) is first integrated forward in time with an initial guess of the control variables, $u_i, i = 1, 2, 3$. Next, the adjoint system (37) is integrated backward in time using the computed state trajectories and the current control values. The controls are then updated point-wise by applying the formulas derived in (39), ensuring that they remain within the admissible bounds. This forward–backward process is repeated iteratively until convergence is achieved, thereby yielding the optimal state, adjoint, and control trajectories that satisfy the necessary conditions for optimality. The numerical algorithm for the optimal control problem is given in the Appendix.

Figures 9 and 10 present the optimal system and the corresponding optimal controls. In Figure 9, we compare the system dynamics with and without control. The results show that the optimal system performs better, as it reduces the overall cost of treatment, minimizes side effects, and lowers the level of infection. Figure 10 presents the control functions. The results indicate that treatment doses should be administered at higher levels initially and then gradually reduced over time. This dosing strategy helps to suppress infection effectively while also minimizing treatment costs and potential side effects.

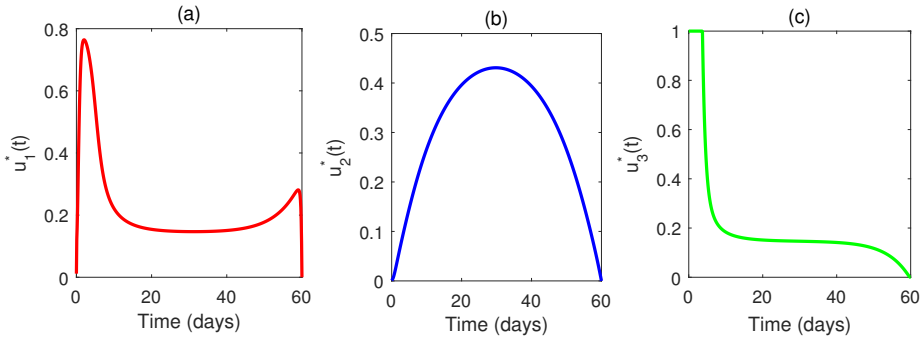

Figure 10. Control functions are plotted. Parameter values are taken from Figure 9.

From the numerical simulations of the optimal control problem, we find that the optimal control approach not only provides a mathematical basis for designing optimal treatment strategy but also offers practical insights into balancing efficacy and cost. The findings suggest that combination therapies, particularly those involving chemotherapy and immune stimulation, represent the most promising pathway toward HPV eradication and cervical cancer prevention.

9. Conclusions and discussion

Cervical cancer is still a serious health problem worldwide. It is mainly caused by long-term infection with HPV. Even though vaccines and treatments have improved, completely removing HPV and stopping its cancer-causing effects remains challenging. Mathematical models and control approaches are useful for testing how different treatments can work together to manage HPV transmission.

In this study, we proposed a new mathematical model using interactions among the susceptible epithelial cells, infected cells, free virions, CTLs, neutralizing antibodies, and cancerous cells. The model was analysed analytically and numerically using MATLAB. Analytically, we found the equilibria and studied their stability. We found two equilibria: DFE and EE. We derived the basic reproduction number (R_0), and showed that the DFE is stable when $R_0 < 1$ and unstable when $R_0 > 1$. At $R_0 = 1$, forward bifurcation occurs. EE is feasible when $R_0 > 1$, and it is globally stable.

Finally, we applied optimal control theory using the maximum principle to focus on optimal combined therapy using chemotherapy ($u_1(t)$), immune system stimulation through CTLs ($u_2(t)$), and antibody therapy ($u_3(t)$). We identified the best treatment strategies that can minimize HPV infection and side-effects. The results showed that combining therapies works better than using them alone. Chemotherapy lowers virus production and kills infected cells, CTL stimulation boosts immune defense, and antibody therapy helps neutralize free viruses. Together, they act in synergy to reduce infection and slow cancer growth. Numerical results suggest that combining chemotherapy with CTL stimulation in short, strong doses can be especially effective, pushing viral levels below persistence thresholds and limiting cancer cell growth. These combinations may improve cancer cell death and reduce resistance to immune-based therapies. Thus, the optimal control approach provides a framework for balancing infection suppression with treatment costs, allowing us to explore the synergistic effects of chemotherapy, immunotherapy, and antibody therapy in HPV management.

The findings from this study provide valuable insights for researchers, highlighting promising

directions for designing treatment strategies that harness both medical and immune system interventions in tandem. Optimizing treatment timing and intensity is key to balancing effectiveness with safety. Future research could adapt this approach to individual patients, include random effects, or use clinical trial data to make the model more relevant for real-world HPV management and cervical cancer prevention. Time delay can be included, and optimal control using the delay model will be more real [31].

Author contributions

Fahad Al Basir: Conceptualization, methodology, software, validation, formal analysis, investigation, writing original draft preparation and writing—review and editing; Konstantin B. Blyuss: Conceptualization, validation, investigation, writing original draft preparation and writing—review and editing; Khalid Aldawsari: Methodology, formal analysis, supervision and project administration. All authors have read and agreed to the published version of the manuscript.

Use of Generative-AI tools declaration

The authors declare that they have not used Artificial Intelligence (AI) tools in the creation of this article.

Data availability statement

The data used here are mention within the article.

Acknowledgements

The authors extend their appreciation to Prince Sattam bin Abdulaziz University for funding this research work through the project number (PSAU/ 2025/01/34088).

Conflict of interest

The authors declare that there are no conflicts of interest.

References

1. J. Wolf, L. F. Kist, S. B. Pereira, M. A. Quessada, H. Petek, A. Pille, et al., Human papillomavirus infection: epidemiology, biology, host interactions, cancer development, prevention, and therapeutics, *Rev. Med. Virol.*, **34** (2024), e2537. https://doi.org/10.1002/rmv.2537
2. D. Hanahan, R. A. Weinberg, Hallmarks of cancer: the next generation, *Cell*, **144** (2011), 646–674. https://doi.org/10.1016/j.cell.2011.02.013
3. E. H. Elbasha, E. J. Dasbach, R. P. Insinga, Model for assessing human papillomavirus vaccination strategies, *Emerg. Infect. Dis.*, **13** (2007), 28–41. https://doi.org/10.3201/eid1301.060438

4. L. Kumar, S. Gupta, Integrating chemotherapy in the management of cervical cancer: a critical appraisal, *Oncology*, **91** (2016), 8–17. https://doi.org/10.1159/000447576
5. M. Xu, C. Cao, P. Wu, X. Huang, D. Ma, Advances in cervical cancer: current insights and future directions, *Cancer Commun.*, **45** (2025), 77–109. https://doi.org/10.1002/cac2.12629
6. S. Dilruba, G. V. Kalayda, Platinum-based drugs: past, present and future, *Cancer Chemother. Pharmacol.*, **77** (2016), 1103–1124. https://doi.org/10.1007/s00280-016-2976-z
7. M. Robati, D. Holtz, C. J. Dunton, A review of topotecan in combination chemotherapy for advanced cervical cancer, *Ther. Clin. Risk Manag.*, **4** (2008), 213–218. https://doi.org/10.2147/TCRM.S1771
8. C. A. Burmeister, S. F. Khan, G. Schäfer, N. Mbatani, T. Adams, J. Moodley, et al., Cervical cancer therapies: current challenges and future perspectives, *Tumour Virus Res.*, **13** (2022), 200238. https://doi.org/10.1016/j.tvr.2022.200238
9. S. Movva, L. Rodriguez, H. Arias-Pulido, C. Verschraegen, Novel chemotherapy approaches for cervical cancer, *Cancer*, **115** (2009), 3166–3180. https://doi.org/10.1002/cncr.24364
10. A. K. Bag, S. Ghosh, A. N. Chatterjee, P. K. Roy, A mathematical framework investigating the impact of Chemo-iPSC therapy for the dynamics of cervical cancer, *J. Appl. Math. Comput.*, **71** (2025), 6061–6093. https://doi.org/10.1007/s12190-025-02476-2
11. R. O. Dillman, Monoclonal antibodies in the treatment of malignancy: basic concepts and recent developments, *Cancer Invest.*, **19** (2001), 833–841. https://doi.org/10.1081/CNV-100107745
12. G. J. Weiner, Building better monoclonal antibody-based therapeutics, *Nat. Rev. Cancer*, **15** (2015), 361–370. https://doi.org/10.1038/nrc3930
13. D. Zahavi, L. Weiner, Monoclonal antibodies in cancer therapy, *Antibodies*, **9** (2020), 34. https://doi.org/10.3390/antib9030034
14. K. Allali, Stability analysis and optimal control of HPV infection model with early-stage cervical cancer, *BioSystems*, **199** (2021), 104321. https://doi.org/10.1016/j.biosystems.2020.104321
15. A. Boukhouima, E. M. Lotfi, M. Mahrouf, S. Rosa, D. F. M. Torres, N. Yousfi, Stability analysis and optimal control of a fractional HIV-AIDS epidemic model with memory and general incidence rate, *Eur. Phys. J. Plus*, **136** (2021), 103. https://doi.org/10.1140/epjp/s13360-020-01013-3
16. J. P. Mateus, P. Rebelo, S. Rosa, C. M. Silva, D. F. M. Torres, Optimal control of non-autonomous SEIRS models with vaccination and treatment, *Discrete Contin. Dyn. Syst. Ser. S*, **11** (2017), 1179–1199. https://doi.org/10.3934/dcdss.2018067
17. S. Chakraborty, X. Z. Li, P. K. Roy, How can HPV-induced cervical cancer be controlled by a combination of drug therapy? A mathematical study, *Int. J. Biomath.*, **12** (2019), 1950070. https://doi.org/10.1142/S1793524519500700
18. A. S. Perelson, P. W. Nelson, Mathematical analysis of HIV-1 dynamics in vivo, *SIAM Rev.*, **41** (1999), 3–44. https://doi.org/10.1137/S0036144598335107
19. R. J. De Boer, A. S. Perelson, Target cell limited and immune control models of HIV infection: a comparison, *J. Theor. Biol.*, **190** (1998), 391–402. https://doi.org/10.1006/jtbi.1997.0548

20. C. D. Murin, I. A. Wilson, A. B. Ward, Antibody responses to viral infections: a structural perspective across three different enveloped viruses, *Nat. Microbiol.*, **4** (2019), 734–747. https://doi.org/10.1038/s41564-019-0392-y

21. G. E. Mahlbacher, K. C. Reihmer, H. B. Frieboes, Mathematical modeling of tumor-immune cell interactions, *J. Theor. Biol.*, **469** (2019), 47–60. https://doi.org/10.1016/j.jtbi.2019.03.002

22. P. Dubey, U. S. Dubey, B. Dubey, Modeling the dynamics of viral–host interaction during treatment of productively infected cells and free virus involving total immune response, *Nonlinear Anal. Model. Control*, **26** (2021), 678–701. https://doi.org/10.15388/namc.2021.26.21434

23. C. Jiang, W. Wang, Complete classification of global dynamics of a virus model with immune responses, *Discrete Contin. Dyn. Syst. Ser. B*, **19** (2014), 1087–1103. https://doi.org/10.3934/dcdsb.2014.19.1087

24. O. Diekmann, J. A. P. Heesterbeek, M. G. Roberts, The construction of next-generation matrices for compartmental epidemic models, *J. R. Soc. Interface*, **7** (2010), 873–885. https://doi.org/10.1098/rsif.2009.0386

25. F. Al Basir, K. B. Blyuss, E. Venturino, Stability and bifurcation analysis of a multi-delay model for mosaic disease transmission, *AIMS Math.*, **8** (2023), 24545–24567. https://doi.org/10.3934/math.20231252

26. S. Lenhart, J. T. Workman, *Optimal control applied to biological models*, Boca Raton, FL: Chapman & Hall/CRC, 2007.

27. L. S. Pontryagin, V. G. Boltyanskii, R. V. Gamkrelidze, E. F. Mishchenko, *The mathematical theory of optimal processes*, New York: Interscience Publishers, 1962.

28. M. Verma, S. Erwin, V. Abedi, R. Hontecillas, S. Hoops, A. Leber, et al., Modeling the mechanisms by which HIV-associated immunosuppression influences HPV persistence at the oral mucosa, *PLoS ONE*, **12** (2017), e0168133. https://doi.org/10.1371/journal.pone.0168133

29. M. A. Nowak, C. R. M. Bangham, Population dynamics of immune responses to persistent viruses, *Science*, **272** (1996), 74–79. https://doi.org/10.1126/science.272.5258.74

30. F. Al Basir, K. B. Blyuss, A. A. Raezah, B. Rahman, H. J. Alsakaji, Mathematical modelling of the role of Langerhans cells in the dynamics of HPV infection, *Sci. Rep.*, **15** (2025), 17505. https://doi.org/10.1038/s41598-025-02608-5

31. C. Liu, Z. Gong, C. Yu, S. Wang, K. L. Teo, Optimal control computation for nonlinear fractional time-delay systems with state inequality constraints, *J. Optim. Theory Appl.*, **191** (2021), 83–117. https://doi.org/10.1007/s10957-021-01926-8

Appendix

Numerical algorithm for the optimal control problem: The optimal control problem is solved numerically using the forward–backward sweep method. To improve numerical stability and reproducibility, both the state and adjoint systems are discretized using the classical fourth-order Runge-Kutta (RK4) scheme on a uniform temporal mesh. The computational procedure is summarized as follows:

(1) **Initialization:**

i. Define all model parameters (e.g., β, k, c, d_A) and control weighting constants B_1–B_3.

ii. Specify the initial conditions

$$S(0),\ I(0),\ V(0),\ C(0),\ E(0),\ A(0).$$

iii. Choose the final simulation time T, uniform time step Δt, maximum iteration number $N_{\max}$, and convergence tolerance ε.

iv. Discretize the interval $[0, T]$ into $N = T/\Delta t$ subintervals.

v. Initialize the control functions using biologically feasible constant guesses:

$$u_1^{(0)}(t) = u_2^{(0)}(t) = u_3^{(0)}(t) = 0, \qquad t \in [0, T].$$

(2) **Forward sweep (state system):**

i. Using the current controls

$$u_1^{(k)}(t),\ u_2^{(k)}(t),\ u_3^{(k)}(t),$$

solve the state system forward in time from $t = 0$ to $t = T$ using the RK4 method.

ii. At each time node, compute and store the numerical approximations of

$$S(t),\ I(t),\ V(t),\ C(t),\ E(t),\ A(t).$$

(3) **Backward sweep (adjoint system):**

i. Impose the transversality conditions

$$\lambda_i(T) = 0, \quad i = 1, 2, \ldots, 6.$$

ii. Solve the adjoint system backward in time from $t = T$ to $t = 0$ using the RK4 method together with the previously computed state variables.

iii. Store the adjoint variables

$$\lambda_S(t),\ \lambda_I(t),\ \lambda_V(t),\ \lambda_C(t),\ \lambda_E(t),\ \lambda_A(t).$$

(4) **Control update:** Update the controls using the characterization obtained from Pontryagin's maximum principle:

$$u_1^{(k+1)}(t) = \max\{0,\ \min(1,\ \frac{\theta_V V(t)\lambda_V(t)}{B_1})\},$$
$$u_2^{(k+1)}(t) = \max\{0,\ \min(1,\ \frac{\theta_C\, C(t)\, \lambda_C(t)}{B_2})\},$$
$$u_3^{(k+1)}(t) = \max\{0,\ \min(1,\ -\frac{\mu\lambda_A(t)}{B_3})\}.$$

To improve convergence stability, the updated controls are relaxed according to

$$u_i^{(k+1)} = \eta\, u_i^{(k+1)} + (1 - \eta)\, u_i^{(k)}, \qquad i = 1,\ 2,\ 3,$$

where $0 < \eta \leq 1$ is the relaxation parameter.

(5) **Convergence test:** Compute the maximum error between successive control iterates:

$$E^{(k)} = \max_{i=1,2,3} \left\| u_i^{(k+1)} - u_i^{(k)} \right\|_\infty .$$

If $E^{(k)} < \varepsilon$, the iterative process is terminated. Otherwise, set

$$k \leftarrow k + 1,$$

and repeat the forward and backward sweeps.

(6) **Output:** The numerical scheme yields the optimal controls $u_1^*(t)$, $u_2^*(t)$, $u_3^*(t)$, together with the corresponding optimal state trajectories

$$S(t),\ I(t),\ V(t),\ C(t),\ E(t),\ A(t).$$

AIMS Press